Body-centric ultra-wideband multi-channel characterisation and spatial diversity in the indoor environment

Published in IET Microwaves, Antennas & Propagation
Received on 13th December 2011
Revised on 29th May 2012
Accepted on 24th July 2012
doi: 10.1049/iet-map.2011.0565

ISSN 1751-8725

Body-centric ultra-wideband multi-channel characterisation and spatial diversity in the indoor environment

Philip A. Catherwood[1], *William G. Scanlon*[1,2]

[1]*Wireless Communications Research Group, The Institute of Electronics, Communications and Information Technology (ECIT), Queen's University Belfast, NI Science Park, Queen's Road, Queen's Island, Belfast BT3 9DT, UK*
[2]*Telecommunication Engineering, University of Twente, Enschede, The Netherlands*
E-mail: w.scanlon@qub.ac.uk

Abstract: This study presents the findings of an empirical channel characterisation for an ultra-wideband off-body optic fibre-fed multiple-antenna array within an office and corridor environment. The results show that for received power experiments, the office and corridor were best modelled by lognormal and Rician distributions, respectively [for both line of sight (LOS) and non-LOS (NLOS) scenarios]. In the office, LOS measurements for t_{mean} and t_{RMS} were both described by the Normal distribution for all channels, whereas NLOS measurements for t_{mean} and t_{RMS} were Nakagami and Weibull distributed, respectively. For the corridor measurements, LOS for t_{mean} and t_{RMS} were either Nakagami or normally distributed for all channels, with NLOS measurements for t_{mean} and t_{RMS} being Nakagami and normally distributed, respectively. This work also shows that achievable diversity gain was influenced by both mutual coupling and cross-correlation co-efficients. Although the best diversity gains were 1.8 dB for three-channel selective diversity combining, the authors present recommendations for improving these results.

1 Introduction

The use of multiple-antenna technology to achieve performance improvements such as increased bandwidth, throughput, diversity gain, is increasing in popularity [1]. However, in body-centric applications the nature of the wearable array topology is such that the user's body influence can lead to higher levels of antenna-to-antenna interactions and for most scenarios the number of antennas and the maximum element spacing is restricted by the physical size of the wearer [2]. It is predicted that future technology developments will lead to dramatic increases in body-worn communication devices [3, 4]. Thus, it is essential to understand the ultra-wideband (UWB) radio propagation channel for particular environments and antenna topologies by undertaking characterisation of the radio channel.

UWB is a technology developed to transfer large amounts of data wirelessly over short distances (typically < 10 m), operating by transmitting signals over a very wide spectrum of frequencies [5] and very low-power spectral density, making it ideal for short-range high-speed personal area and body area networks (BANs) [6]. UWB systems inherently exhibit less fading than their narrowband counterparts because of short pulse length UWB transmissions, making signals more robust to multipath fading [7, 8]. One of the key goals of multiple-antenna technology is to achieve a diversity gain over single-channel equivalents, with diversity effectiveness of multiple-antenna systems being dependent on the richness of the scattering environment and the fading characteristics of the channel [9]. Multiple-antenna technology is traditionally used for narrowband systems to alleviate the effects of multipath fading [10]. UWB already has inbuilt frequency diversity because of its large bandwidth; however, spatial diversity offers improved radiation capture through spatial arrangement of multiple antennas [7].

Multiple-antenna UWB systems having been trialled successfully for non-body-worn applications [10, 11] and results show increases in link robustness [12, 13]. There have been a small number of researchers exploring the area of multiple-antenna UWB systems for wireless personal area networks including Farserotu *et al.* [9], Al-Qaraawy and Ali [14] and Dong *et al.* [15]. However, none of the work to date has addressed the issue of body-mounted UWB multiple antennas for the off-body links required for personal area networks, despite it being fundamental to the development of many systems including backhaul and connectivity support for BANs. Furthermore, all of the research to date was based on radiofrequency (RF) cable measurements for the body-centric antenna array and many used static frequency-domain measurements, which fail to facilitate real-time capture of dynamic natural user movements.

For the first time, this paper investigates off-body UWB channels for a body-centric fibre optic-fed multi-antenna transmitter and a wall-mounted base station in an office and corridor environment, and also investigates mutual coupling effects on received power and diversity gain when antennas

are mounted on the human body and selective diversity channel combination techniques are employed, offering mathematical modelling in each case.

This work utilises empirical data collection, which has advantages over computer simulation (such as ray tracing). Simulations, while being a very useful tool in channel characterisation, cannot faithfully capture the natural movements of the human body for body-centric mobile radio systems. Furthermore, simulation accuracy is dependent on the quality of the model (permittivity values, specification of geometry) and the nature of the assumptions made on the electromagnetic side.

The remainder of the paper is structured as follows. Section 2 outlines the measurement system and the measurement procedure and methodology. Received signal characteristics and delay statistics are presented in Section 3. The paper concludes with a discussion of the results obtained and some brief recommendations for further work.

2 Experimental procedure

2.1 Measurement system

For body-centric UWB communications, uncontrollable events such as shadowing from the torso, moving limbs, changes in orientation and pedestrians in close proximity will all serve to create temporal variation in both received power and delay characteristics. Therefore it is important to perform dynamic measurements that incorporate typical operating conditions such as natural walking movements, including swinging arms, torso rotation and so on. As fully synchronised time-domain multiple-antenna sounders are very expensive to implement [16], the most popular multiple-antenna sounding technique is the use of a sequential sounder [17], which utilises a single channel sounder in conjunction with a sequentially switched antenna array [18]. This system sequentially measures the complex single-in single-out impulse responses between all the combinations of the transmitters and receivers, and the combination of these SISO impulse responses give the complex multiple-antenna system impulse response [19].

A multiple-antenna measurement system was implemented as shown in Fig. 1*a*. The UWB source was a PulsON P210 system [www.timedomain.com] and was fed into an RF/optical link [http://www.miteq.com] [http://www.linphotonic.com/documents/Datasheets/miniPR.pdf], implemented to reduce measurement errors induced through the movement of RF reflective cabling used to feed the body-centric antennas which naturally move during dynamic testing, as reported in [20]. The UWB source had a centre frequency of 4.7 GHz, bandwidth of 3.2 GHz and launch power of −12 dBm. When the optical signal was converted into an RF signal, it was then fed into a broadband SP4T high-speed switch (HMC345LP3) [http:// www.hittite.com/content/documents/data_sheet/hmc345lp3.pdf] and time-interleaved to three vertically-polarised UWB transmit antennas (Fractus, UM-FR05-S1-P-0-107 [http://www.fractus.com/main/fractus/srw_3.1/]), with the fourth RF port having a 50 Ω load to enable an accurate time reference by providing a notch in the received time series.

The transmit time on each channel was 10 ms, with a full cycle through all four channels lasting for 40 ms with a switching speed between channels of 50 ns. A PulsON receive station received the transmitted packets with a vertically polarised PulsON P200 Broadspec UWB antenna [http://www.timedomain.com] with the antenna orientated broadside towards the user. Data were then transferred to a

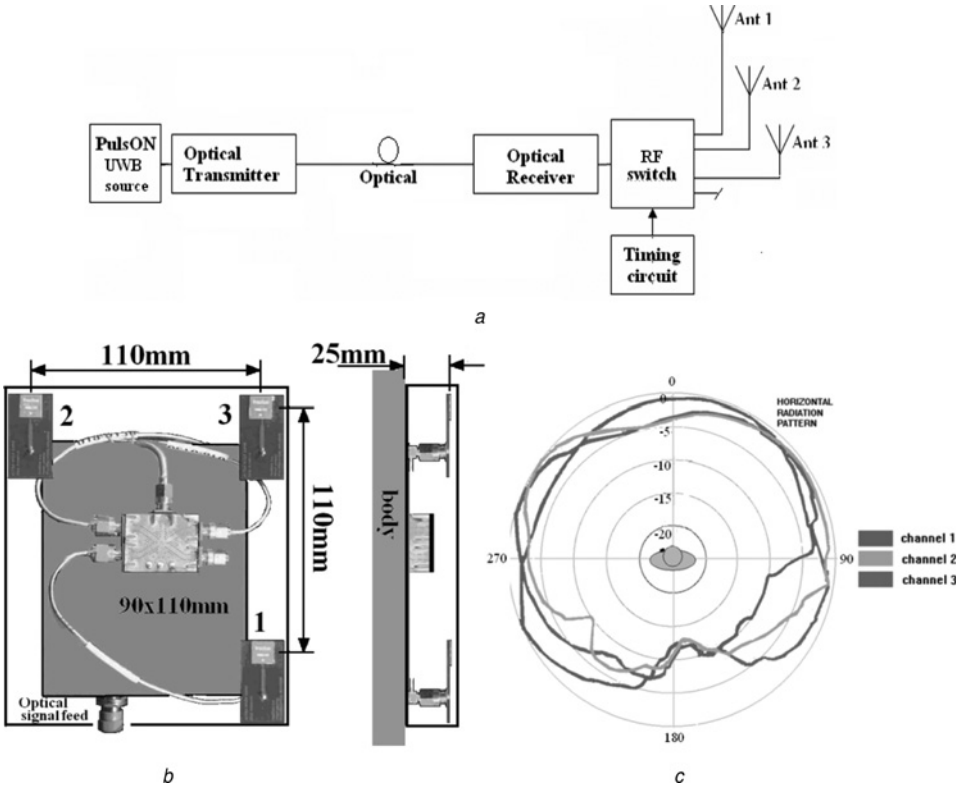

Fig. 1 *UWB transmitter*

a Transmitter block diagram
b Body-worn optical measurement system (photograph re-touched for clarity)
c Measured azimuthal radiation patterns for chest-mounted array (recorded mid-band at 4.7 GHz)

doi: 10.1049/iet-map.2011.0565

laptop for storage. The propagation channel was sampled at a rate of 100 scans per second, thus each channel was sampled at 25 Hz (the Doppler frequency for such a mobile transmitter is 10 Hz). A frequency-domain technique was employed to de-convolve the measurement systems from the received signal, leaving only the transfer function of the propagation channel. This required the recording of a reference measurement within an RF anechoic chamber.

During testing, the PulsON UWB signal source and the RF/optical converter were carried in a waist-mounted rear facing holster. The miniature optical receiver (optical to RF converter), timer and the RF channel switch were housed in a small plastic enclosure, mounted on the user's chest and had its own miniature power supply.

2.1.1 Antenna separation distance: Both the spatial diversity gain and the correlation between channels of a multiple-antenna system is a function of the antenna separation distance, with correlation generally decreasing as the separation distance increases [21]. A theoretical relationship between spatial correlation and spatial antenna spacing is described by [22]

$$\rho(d) = J_o^2(2\pi d/\lambda) \quad (1)$$

where d is the antenna separation and λ is wavelength (m), J_o is a Bessel function of the first kind of zeroth order. Although large spacing is required to ensure low correlation, for a body-centric application it is often more desirable to have a rectangular geometrical antenna array. It is recommended [23] that two signals are suitably de-correlated if their cross-correlation coefficient (CCC) is of a factor 0.7 or less, allowing maximum theoretical diversity gain to be achieved [24]. To ensure channel correlation is suitably low across the UWB frequency range, antenna separation of >10 cm (one wavelength) will be required [25]. However, work in [25] was undertaken for isolated antennas; no equivalent recommendation for body-centric antennas has been clearly specified in literature. Body-worn systems introduce physical limitations to the antenna spacing because of human body geometry [9]. The UWB antennas were thus arranged as depicted in Fig. 1*b*.

For the transmitter antenna array, the physical positioning of the other antennas in the array will affect the azimuthal radiation pattern of individual antennas. The measured patterns for the isolated antennas displayed an almost isotropic azimuthal radiation pattern (not shown). The chest-mounted antenna array (Fig. 1*c*) highlights the effects of mounting antennas onto the human body, with around 13 dB losses in parts of the radiation pattern.

2.2 Experimental indoor environments

Owing to the dependence on geometry and construction material, the measurements were undertaken in environments that covered popular and commonly researched indoor multipath environments [26–28]. Two environments were selected; firstly a 260 m^2 (21 m × 1.3 m) corridor (Fig. 2*a*) situated on the fifth floor of Block 1 of the University of Ulster (Jordanstown) building, as previously implemented by Ziri-Castro *et al.* [29]. The second location was a 42 m^2 (7 m × 6 m) open-plan modern office (Fig. 2*b*), also on the fifth floor of the same building, as utilised by Catherwood and Scanlon [20].

2.3 Measurement procedure

Tests were subdivided into two categories for each environment: line of sight (LOS) or non-LOS (NLOS), depending on the orientation of the worn antennas with respect to the receive antenna. The base station receiver was positioned at a height of 2 m from the ground for both environments, with their position shown in Figs. 2*a* and *b*. The wearable transmitting antenna array was positioned on the user's chest (1.4 m above floor level) and held against the body using an adjustable synthetic elastic cuff to minimise body–antenna separation during testing, as previously implemented by Fort *et al* [30]. The test user was an adult male of mass 82 kg and height 1.78 m. To minimise spurious reflections all metal objects such as belts, jewellery and coinage were removed from the subject. LOS tests were conducted with the user (and transmitting array) directly facing the Rx antenna and NLOS completed 180° from the LOS position (directly facing away). Tests were conducted in the office environment for a linear path from 8 to 2 m Tx–Rx separation (LOS) with the transmitter moving at 0.5 m/s, and then for a return journey (NLOS) using the same walking speed and path. In the corridor, a linear path from 10 to 2 m Tx–Rx separation (LOS) was traversed with the mobile transmitter moving at a linear speed of 0.5 m/s, and the return journey (NLOS) also conducted.

3 Experimental results

To facilitate an in-depth investigation of body-centric UWB multiple antennas, the power and delay statistics of the

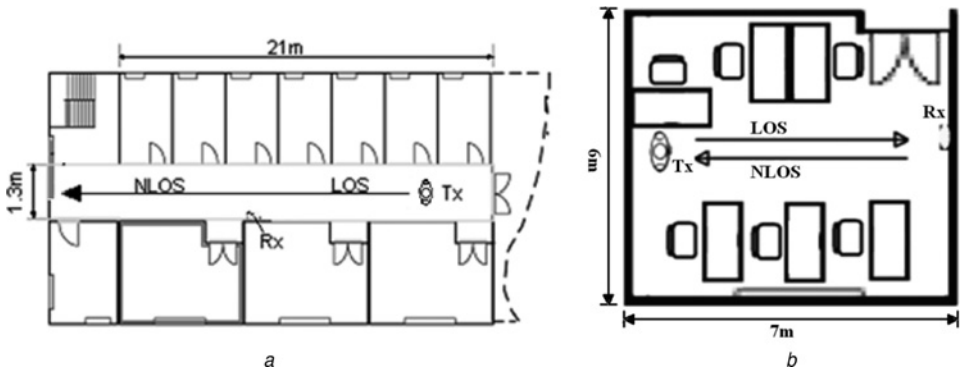

Fig. 2 *Measurements environments*

a Office block corridor
b Open plan office

received signals were studied to analyse each multiple-antenna channel in turn. In addition, the receive diversity gains for a selective diversity scheme were evaluated. Mean delay (t_{mean}, the first central moment of the power delay profile) and root-mean-square (RMS) delay spread (t_{RMS}, the average propagation delay relative to the first-arriving signal component) are instrumental in describing wideband fading [31]. The total received wideband power can be determined by the sum of the squares of all the amplitudes in the PDP [32]. To prevent noise from affecting calculated delay statistics, a threshold was incorporated into the signal processing software to give most accurate results for t_{mean} and t_{RMS} values, as reported by Wong *et al.* [33].

3.1 Received power tests

Measurements were first taken for the antenna array mounted on a wooden stand positioned at a height of 1.4 m from the floor and a distance of 3.2 m from the receive antenna. Each measurement was recorded over a 5 s period (500 distinct PDPs), and then the power and delay results were averaged over this time.

The results in Table 1 show that the three antennas had similar power and delay values, with variation because of the antenna positioning in the array. The powers in the office were higher than for the corridor, and the values for both mean delay and RMS delay spreads were less for the office than the corridor.

To mathematically describe the channel parameters, for each scenario the maximum likelihood (ML) estimates of received UWB signal amplitude were calculated for popular statistical distributions and the Akaike information criterion (AIC) was used to select the closest fitting distribution.

Table 1 Received power and delay statistics for the isolated antenna array (LOS)

		Channel		
		1	2	3
office	power, dBm	−65.2	−64.9	−65.7
	t_{mean}, ns	16.9	15.8	16.3
	t_{RMS}, ns	22.1	21.4	23.1
corridor	power, dBm	−68.3	−67.9	−69.2
	t_{mean}, ns	24.7	24.5	25.2
	t_{RMS}, ns	31.8	31.4	32.3

The results of received power (Table 2) in the office show that all three channel distributions are described by the lognormal distribution, as predicted by Chong *et al.* [34], with reasonably similar statistical parameters. All three channel distributions for the corridor-received power measurements are described by the Rician distribution. Rice has been traditionally considered for LOS arrangements because of a dominant component, but NLOS was also Rician in this situation because of high wave guiding of radiated power along the corridor (possibly a reflection of the dominant ray off the opposite end of the corridor).

Analysis of Fig. 3*a* depicts that each of the three channels displays similar power loss characteristics for the LOS office journey. For NLOS office environment (Fig. 3*b*) it is observed that two of the three channels had similar shadowing characteristics, whereas one channel experienced more power loss (channel 1). For the LOS corridor journey (Fig 3*c*), channel 2 had less power loss than channels 1 or 3. For the NLOS corridor configuration (Fig. 3*d*), channel 3 had the least and channel 1 had the most power loss. Also, the NLOS results displayed a larger range than LOS results for all channels.

3.2 Time delay

3.2.1 Mean delay and standard deviation:

Examination of Fig. 4 reveals first that t_{mean} and t_{RMS} LOS delays were less than t_{mean} and t_{RMS} NLOS delays, and t_{mean} and t_{RMS} delays in the office were less than t_{mean} and t_{RMS} delays in the corridor. This is because LOS scenarios have less shadowing and reflection than NLOS; also the office had a lower reflection order than the corridor. Furthermore, standard deviation for LOS was generally less than NLOS in both environments for t_{mean} and t_{RMS} and standard deviation for office is less than for corridor. This was again because of higher reflections in the corridor environments and increased NLOS shadowing because of human body movement.

3.2.2 Time-delay cumulative distribution functions:

ML estimates and the AIC were again used to select the closest fitting distribution. In the office, LOS measurements for t_{mean} and t_{RMS} were both described by the Normal distribution for each of the three channels, and NLOS measurements for t_{mean} and t_{RMS} were modelled by the Nakagami and Weibull distributions, respectively, for all three channels (Table 3). For the corridor measurements,

Table 2 Received power results for the body-worn antenna array and statistical parameters

			Received power, dBm	Signal range, dB	Distribution	Statistical parameters			
						μ		σ	
						Est.	Std. Err.	Est.	Std. Err.
office	1	LOS	−61.7	5.2	lognormal	−0.00046	0.00106	0.01056	0.00075
		NLOS	−74.6	10.8	lognormal	−0.00013	0.00082	0.01354	0.00058
	2	LOS	−61	5.8	lognormal	0.00012	0.00105	0.01045	0.00074
		NLOS	−76.4	9.4	lognormal	−0.00036	0.00138	0.02274	0.00098
	3	LOS	−62.6	5.4	lognormal	−0.00048	0.00121	0.01215	0.00087
		NLOS	−74.2	8.8	lognormal	−0.00055	0.00131	0.02149	0.00093
corridor	1	LOS	−64.4	13.5	Rician	$s = 1.0002$	$s = 0.0012$	0.01545	0.00086
		NLOS	−72.6	15.1	Rician	$s = 0.9980$	$s = 0.0004$	0.01635	0.00028
	2	, LOS	−62.9	8.6	Rician	$s = 1.0008$	$s = 0.0012$	0.01526	0.00085
		NLOS	−73.7	15.3	Rician	$s = 0.9973$	$s = 0.0006$	0.0237	0.0004
	3	LOS	−63.5	11.3	Rician	$s = 1.0008$	$s = 0.0012$	0.01506	0.00084
		NLOS	−72.8	14.2	Rician	$s = 0.9990$	$s = 0.0006$	0.02656	0.00045

doi: 10.1049/iet-map.2011.0565

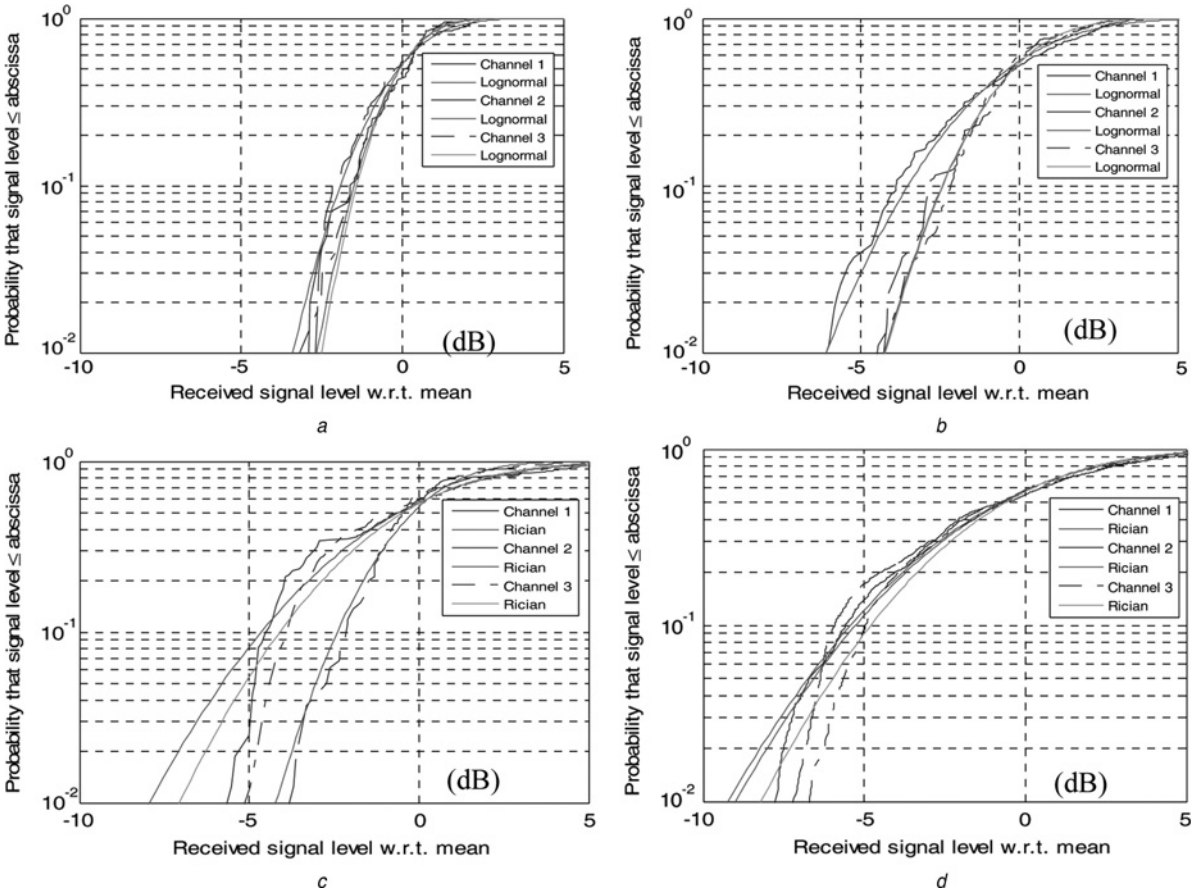

Fig. 3 *CDFs of received power*

a Office LOS
b Office NLOS
c Corridor LOS
d Corridor NLOS
Distribution parameters are provided in Table 2

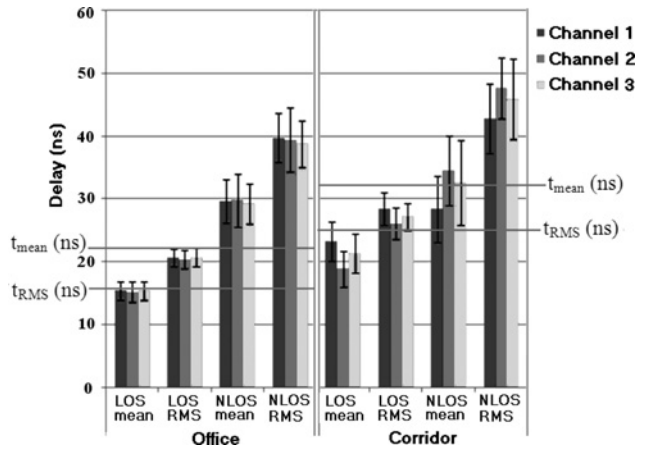

Fig. 4 *Mean delay values and standard deviation (t_{mean} and t_{RMS} values for isolated antenna shown as horizontal lines)*

LOS for t_{mean} and t_{RMS} were both described by the Normal distribution for all three channels, except for the t_{mean} measurement for channel 3, which was Nakagami distributed (Table 3). On this occasion, there were only small differences between the Nakagami and Normal distributions; however, the Nakagami offered a marginally better fit, as prescribed by the AIC criterion. NLOS measurements for t_{mean} and t_{RMS} were modelled by the Nakagami and Normal distributions, respectively, for each of the three channels.

An analysis of the cumulative distribution functions (CDFs) for t_{mean} and t_{RMS} for the two environments in LOS and NLOS configurations was undertaken (Figs. 5*a*–*h*). It was observed that for the office all three channels had similar t_{mean} and t_{RMS} values for LOS (Figs. 5*a* and *b*), with little difference between the distributions over the LOS journey. For NLOS all three channels had similar t_{mean} and t_{RMS} values with a slight spread in distributions observable (Figs. 5*c* and *d*).

For the LOS distribution in the corridor (Figs. 5*e* and *f*), the distributions of the three channels were slightly spread but had similar shape to each other for both t_{mean} and t_{RMS} values. For the NLOS distributions for the corridor (Figs. 5*g* and *h*), the three channels were notably spaced for both t_{mean} and t_{RMS} values; also t_{mean} and t_{RMS} values for NLOS were larger than LOS for both environments and delays for corridor were larger than for office for both t_{mean} and t_{RMS} delay parameters.

In summary, the delay parameters of the distributions of the individual channels were similar for LOS scenarios and for the office environment. However, for the corridor and particularly for the corridor NLOS arrangement the

Table 3 Time-delay statistical parameters

			Time	Distribution	μ		σ	
					Est.	Std. Err.	Est.	Std. Err.
office	1	LOS	t_{mean}, ns	normal	15.4	0.1	1.4	0.1
			t_{RMS}, ns	normal	20.7	0.1	1.4	0.1
		NLOS	t_{mean}, ns	Nakagami	18.8	—	8.9×10^{-16}	—
			t_{RMS}, ns	Weibull	$a = 41.4$	$a = 0.2$	$b = 12.5$	$b = 0.6$
	2	LOS	t_{mean}, ns	normal	15.1	0.2	1.7	0.1
			t_{RMS}, ns	normal	20.3	0.1	1.5	0.1
		NLOS	t_{mean}, ns	Nakagami	13.1	—	9.0×10^{-16}	—
			t_{RMS}, ns	Weibull	$a = 41.6$	$a = 0.3$	$b = 8.8$	$b = 0.4$
	3	LOS	t_{mean}, ns	normal	15.4	0.2	1.9	0.1
			t_{RMS}, ns	normal	20.7	0.2	2.1	0.1
		NLOS	t_{mean}, ns	Nakagami	21.2	—	8.7×10^{-16}	—
			t_{RMS}, ns	Weibull	$a = 40.4$	$a = 0.2$	$b = 12.1$	$b = 0.6$
corridor	1	LOS	t_{mean}, ns	normal	23.2	0.2	3.1	0.2
			t_{RMS}, ns	normal	28.4	0.2	2.6	0.1
		NLOS	t_{mean}, ns	Nakagami	7.2	—	8.3×10^{-16}	—
			t_{RMS}, ns	normal	42.8	0.1	5.5	0.1
	2	LOS	t_{mean}, ns	normal	18.9	0.2	2.8	0.2
			t_{RMS}, ns	normal	26.0	0.2	2.5	0.1
		NLOS	t_{mean}, ns	Nakagami	9.7	—	1.2×10^{-15}	—
			t_{RMS}, ns	normal	47.7	0.2	4.9	0.1
	3	LOS	t_{mean}, ns	Nakagami	21.4	0.2	3.1	0.2
			t_{RMS}, ns	normal	27.2	0.2	2.2	0.1
		NLOS	t_{mean}, ns	Nakagami	5.9	—	1.1×10^{-15}	—
			t_{RMS}, ns	normal	46.0	0.2	6.4	0.1

channels experienced differing delays, although they were still modelled by the same distributions with mostly differing parameters.

3.3 Antenna mutual coupling, channel cross-correlation and antenna spatial diversity

Diversity schemes can play a key role in addressing fading and shadowing effects in the indoor radio environment; one such popular scheme is spatial diversity. In addition, there are a number of received signal combining methods which may be used to improve the signal-to-noise ratio (SNR) at the output stage of the receiver. One of the most widely used and simplistic combining techniques is selection diversity, which uses selection of the channel with the highest instantaneous SNR [35]. Khaleghi [36] highlights diversity gain as the key performance factor characterising a diversity system, with performance depending on antenna de-correlation [37].

3.3.1 Investigation of the effects of antenna mutual coupling: Measurement of mutual coupling of the antennas in the body-worn array can assist in a better understanding of variations in the results of what are essentially similar antenna systems. Table 1 and Fig. 4 highlight the small degree of variation of power and delay for non-body-worn against body-worn antennas over a typical dynamic path. Mutual coupling between the elements is likely to affect any measured results. Mutual coupling was evaluated in an anechoic chamber using a vector network analyser (Rohde and Schwarz ZVB-8) and measured at the central frequency of the UWB system (4.7 GHz). These results were recorded for the antenna array mounted on the chest, and also for an isolated scenario. Observing Fig. 6*a*, channel 3 experiences mutual coupling effects from antenna 1 below it and antenna 2 to the side. The other two antennas will have less mutual coupling effect because of the diagonal arrangement of antennas 1 and 2. It is also noted that the human body reduces mutual coupling between antennas compared with when the array is isolated from the body.

3.3.2 Channel cross-correlation and antenna spatial diversity: Cross-correlation is a measure of similarity between channels. For a diversity scheme to be effective, each antenna element should receive statistically independent versions of the transmitted signal [38]. The envelope CCC, ρ_c, between the fading envelopes (branch 1) r_1 and (branch 2) r_2 consisting of N samples may be represented by

$$\rho_c = \frac{\sum_{i=1}^{N} [r_1(i) - \bar{r}_1][r_2(i) - \bar{r}_2]}{\sum_{i=1}^{N} [r_1(i) - \bar{r}_1]^2 [r_2(i) - \bar{r}_2]^2} \quad (2)$$

where i is the instantaneous sample value, $\overline{r_1}$ and $\overline{r_2}$ are the respective means of the signal envelopes [39]. It is also possible to consider the reciprocity of the channels, where transmitters and receiver can have their positions reversed with the channel transfer function remaining the same, as confirmed by Dong *et al.* [15] and Qiu *et al.* [40]. Hence, there is the opportunity to examine the potential benefits of employing receive diversity (assuming three receivers on body and the transmitting base station) and also investigate the effects of having antennas close together in a rectangular body-centric package.

Observing Fig. 6*b*, it is first highlighted that all of the envelope CCCs for the UWB channels in the office and corridor environments were < 0.7, the target threshold recommended by Jakes [23]. In addition, it can be seen that the CCCs for LOS were higher than for NLOS arrangements in both environments, as NLOS relies on multipath propagation, which reduces channel correlation [9, 41]. LOS has a more direct path and as such, correlation is higher as neighbouring channels are more likely to experience similar propagation journeys.

From these results, there appears a clear trend between relative antenna location and the channel correlation values.

doi: 10.1049/iet-map.2011.0565

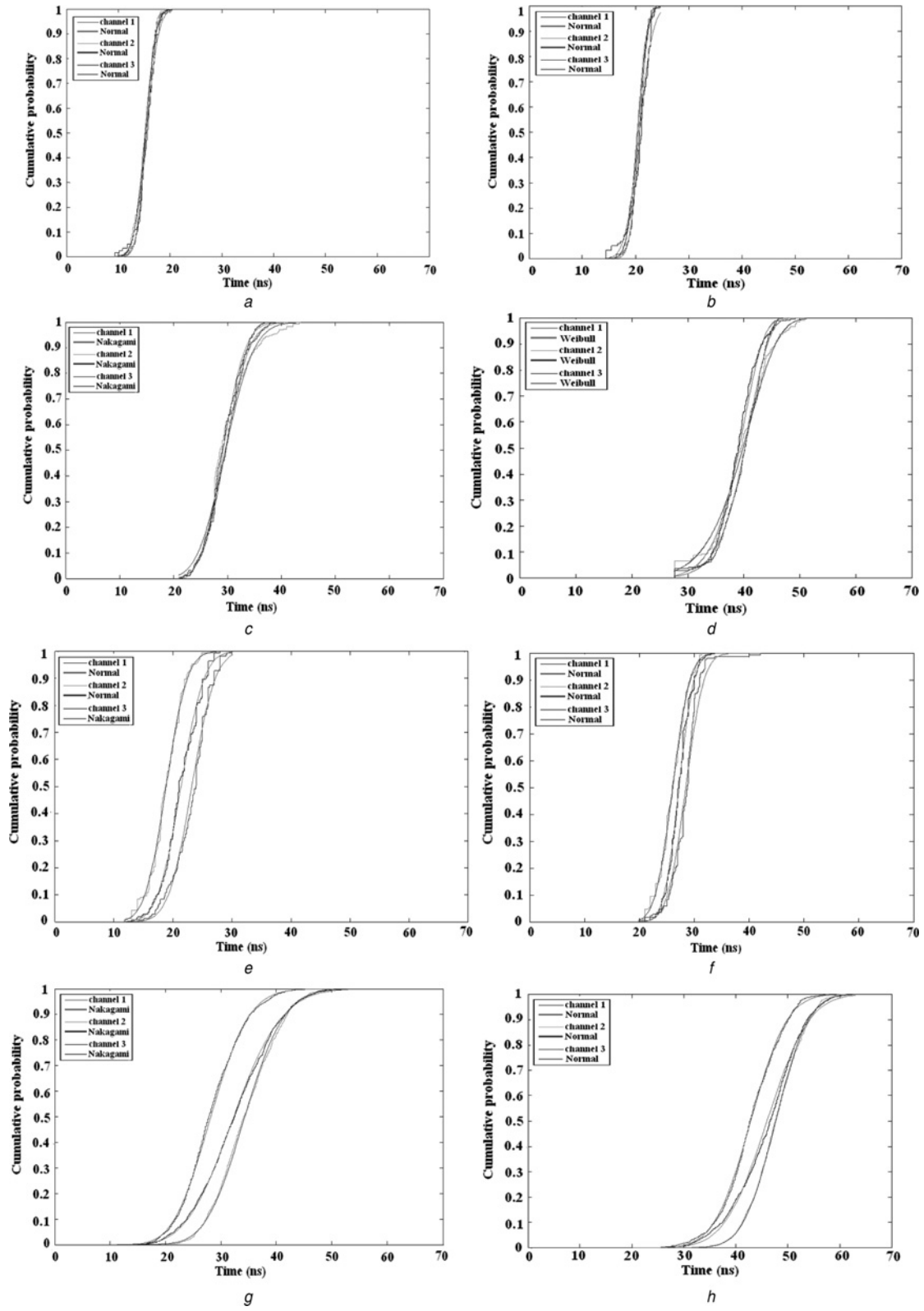

Fig. 5 *CDFs of mean time-delay and RMS delay spread*

a Office LOS mean
b Office LOS RMS
c Office NLOS mean
d Office NLOS RMS
e Corridor LOS mean
f Corridor LOS RMS
g Corridor NLOS mean
h Corridor NLOS RMS

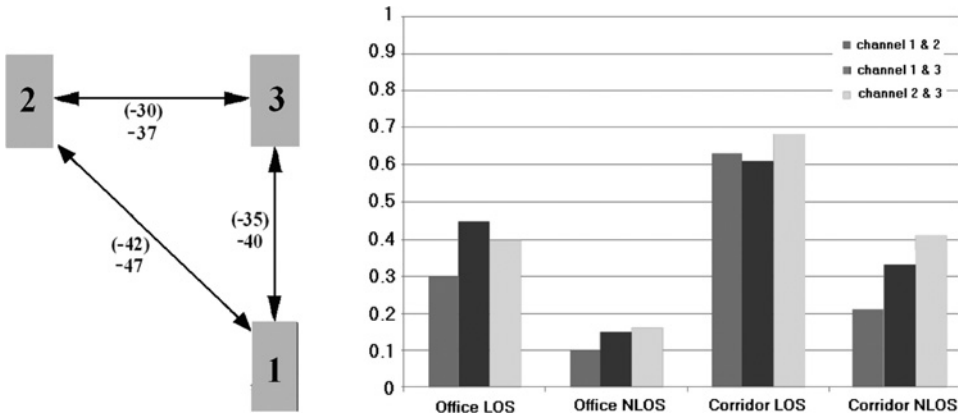

Fig. 6 *Investigation of the effects of antenna mutual coupling*

a Values (in dB) of mutual coupling for a chest-worn array measured in an anechoic chamber (isolated array values shown in brackets)
b Cross-correlation coefficient for each channel combination

Antennas 1 and 2 are diagonally positioned, possibly keeping the CCC to a lower level.

3.3.3 Statistical parameters for combining of signals: ML estimates of the combined received signal statistical parameters and the AIC were used to select the closest fitting distribution. Observing Table 2, each of the three channel distributions for the office environment was described by the lognormal distribution, agreeing with results attained by Chong *et al.* [34]. After combining various two-channel computations using selection diversity, all resultant combined signals remained best described by the lognormal distribution (Table 4). Indeed, combining all three channels using selection diversity resulted in the new signal also being best described by the lognormal distribution (Table 4).

Table 2 highlighted that the channels for the corridor measurements were individually described by the Rician distribution. However, after combining two branches, all resultant signals were now described by the lognormal distribution [except the NLOS channels 1 and 2 combination which is still described by the Rician distribution (Table 4)]. Further combining of all three branches resulted in the signal being described by the lognormal distribution (Table 4). The results from the corridor show that use of combining techniques can change the best fit statistical distribution model for the resultant received signal envelope. The purpose of spatial diversity is to improve overall SNR by reducing the occurrence of significant fading events for a particular link. Therefore it is entirely likely that this reduction in occurrence of low signal levels in the combined envelope results in changes in statistical parameters [42], to the point that the resultant is best described by a different statistical model.

Diversity gain was calculated at 90% wideband signal reliability, as per [39]. Observation of Table 5 shows the 90% signal reliability power levels for the single channels in the LOS office scenario were all approximately similar. Two- and three-channel diversity results showed some advantage over the signal fading characteristics of the single channels. A similar trend in results was seen for the NLOS office measurements. All diversity gains are referenced with respect to the received power on the highest powered channel in the combination.

The 90% signal reliability power levels for the single channels in the LOS corridor scenario had some variations. Interestingly, the 90% signal reliability levels for two- and three-channel combining were similar to the 90% signal

Table 4 Statistical parameters for antenna diversity

			Average power, dBm	Distribution	Statistical parameters			
					μ		Σ	
					Est.	Std. Err.	Est.	Std. Err.
office	1 and 2	LOS	−60.7	lognormal	0.00551	0.00094	0.00941	0.00067
		NLOS	−72.3	lognormal	0.00871	0.00102	0.01674	0.00072
	1 and 3	LOS	−61.6	lognormal	0.00440	0.00102	0.01024	0.00073
		NLOS	−73.5	lognormal	0.00674	0.00104	0.01709	0.00074
	2 and 3	LOS	−61.0	lognormal	0.00673	0.00095	0.00949	0.00068
		NLOS	−74.2	lognormal	0.00858	0.00131	0.02155	0.00093
	1, 2 and 3	LOS	−60.7	lognormal	0.00836	0.00094	0.00936	0.00067
		NLOS	−73.4	lognormal	0.01281	0.00111	0.01824	0.00079
corridor	1 and 2	LOS	−62.6	lognormal	0.00765	0.00111	0.01406	0.00079
		NLOS	−72.1	Rician	$s = 1.00858$	$s = 0.00044$	0.01809	0.00031
	1 and 3	LOS	−63.3	lognormal	0.00733	0.00109	0.01383	0.00077
		NLOS	−71.8	lognormal	0.01069	0.00046	0.01918	0.00033
	2 and 3	LOS	−62.3	lognormal	0.00964	0.00097	0.01232	0.00069
		NLOS	−72.1	lognormal	0.01288	0.00051	0.02114	0.00036
	1, 2 and 3	LOS	−62.2	lognormal	0.01212	0.00101	0.01283	0.00072
		NLOS	−71.5	lognormal	0.01700	0.00044	0.01829	0.00031

doi: 10.1049/iet-map.2011.0565

Table 5 Received power at 90% signal reliability for single antennas and two- and three-branch antenna arrays

			Received power, dBm			Power after combination, dBm			
			1	2	3	1 and 2	1 and 3	2 and 3	1 and 2 and 3
office	LOS	90%	−63.2	−62.9	−64	−62.4	−62.9	−62.3	−62.2
	NLOS	90%	−78.2	−79.1	−76.2	−76.9	−75.8	−76.1	−75.8
corridor	LOS	90%	−68.2	−64.7	−66.7	−64.7	−66.7	−64.7	−64.7
	NLOS	90%	−77.4	−78.8	−77.1	−76.3	−76.3	−76.3	−75.3

reliability levels for channel 2 before selection diversity techniques were employed. For the NLOS office measurements, it was observed that the single channels are similar to each other and two-channel diversity increased the 90% signal reliability level by 1 dB, and three-channel diversity raised it by another 1 dB.

Overall, for both environments it was found that diversity gain was greater for NLOS configurations than for LOS arrangements, because of high shadowing effects increasing diversity of the channel paths. Gesbert and Akhtar [41] advise that for strong transmit correlations or high Rician factors (LOS), the capacity of the multiple-antenna system will essentially become similar to that of a single antenna system. With reference to Fig. 6*a* and Table 5, it is clearly observed that for each environment and LOS/NLOS configuration there is a general correlation between higher values of CCC and lower diversity gains, with the converse also being true, as supported by Farserotu *et al.* [9].

4 Discussion

The presented channel characterisation results cover various combinations and permutations of the two environments (medium multipath rooms and corridors) and LOS/NLOS configurations. Although these scenarios and their associated channel models may not be applicable to larger indoor environments such as conference halls, or where a high density of pedestrians exist, they do represent a reasonable range of conditions relevant to indoor body-centric UWB applications.

4.1 Power

The results showed that the received power is mostly affected by body shadowing. Comparison between the two environments showed that mean received power in the corridor was less than the office for LOS scenarios, but greater for NLOS scenarios. Also, the difference between the average LOS and NLOS received power was found to be less in the corridor, typically because of the lack of furniture to scatter the radio waves in the corridor and also the corridor's tendency to act as a waveguide [43]. However, the range of received power in the corridor was greater than for the office because of the greater number of reflections in the corridor environment. It was generally found that channel 3 had higher received powers and channel 1 had lower powers. Channel 3 was positioned on the top right-hand side of the array (as per Fig. 2) and thus mutual coupling from antennas 1 and 2 affected channel 3's received power at low signal levels.

4.2 Delay

It was seen that the presence of the body in close proximity to the antenna array increased both t_{mean} and t_{RMS} compared with the isolated antenna, because of increased scattering and reflection from the body, particularly because of moving limbs. LOS delays (both t_{mean} and t_{RMS}) were less than those for NLOS, because body shadowing causes the launched signal to rely on reflection and scattering to reach the receiver, and thus multiple delay paths. The office delays (t_{mean} and t_{RMS}) were less than for the corridor, as corridors have high-order reflectivity modes which cause increased delay spreads. Standard deviation of delay was also highest for the NLOS corridor set-up because of increased shadowing because of limb movement in a narrow corridor and the corridor's high-order reflectivity modes increasing the signal spread [24].

4.3 Antenna coupling and signal combining

In the office, all the received power distributions were modelled by the lognormal distribution for both LOS and NLOS and continued to be described by this distribution after channel combining techniques were used. However, when spatial diversity techniques and channel combining strategies were employed in the corridor, statistical distributions mostly changed from Rician to lognormal. It was also discovered that the best diversity gains of 1.3 dB for two-channel combining and 1.8 dB for three-channel combining with respect to the highest received channel power were achievable. These values are for NLOS situations, where it is typically most required in practice. When the UWB antenna array was placed on the human body, it appears not to enjoy the same diversity gains as the non-body-worn equivalents reported in the literature [44, 45]. However, larger antenna array spacing or repositioning of the antennas onto the extremities (arms legs, etc.) may yield greater diversity gains.

The use of three-antenna diversity made a notable difference for NLOS conditions in the corridor environment. In all other circumstances tested the extra complexity of three-antenna diversity did not justify the added complexity.

5 Conclusion

A characterisation of an off-body transmit antenna array in an indoor environment has been presented. As each channel in the sounder was sampled at a rate faster than the Doppler Nyquist frequency and for the same physical and environmental conditions, measurements could be directly compared. The results have underlined the differences in LOS and NLOS configurations and for the two chosen environments. The effects of mutual coupling on the antenna array were highlighted. Also, combining the received signals using selection diversity techniques altered the shadowing distribution characteristics compared with those for the single channels. Combining two received channels yielded small diversity gains in the region of 1 dB, whereas the use of three antennas instead only made a

notable difference for NLOS conditions in the corridor environment. Future work will seek to improve on these results by introducing more sophisticated array arrangements including the use of polarisation diversity.

6 References

1 Cho, Y., Kim, J., Yang, W., Kang, C.L.: 'MIMO-OFDM wireless communications with MATLAB' (Wiley–IEEE Press, 2010)
2 Hanlen, L., Minyue, F.: 'Capacity of MIMO channels: a volumetric approach'. IEEE Int. Conf. on Communications ICC'03, 2003, vol. 5, pp. 3001–3005
3 Cotton, S.L., Conway, G.A., Scanlon, W.G.: 'A time-domain approach to the analysis and modeling of on-body propagation characteristics using synchronized measurements at 2.45 GHz', *IEEE Trans. Antennas Propag.*, 2009, **57**, (4), pp. 943–955
4 Hall, P.S., Hao, Y.: 'Antennas and propagation for body-centric wireless communications' (Artech House, USA, 2006)
5 Ofcom Office of Communications 'Ultra Wideband'. This document consults on a position to adopt in Europe on ultra wideband devices in 3.1–10.6 GHz. Consultation document. Issued: 13 January 2005
6 Allen, B., Ghavami, M., Armogida, A., Aghvami, A.H.: 'The holy grail of wire replacement', *IEEE Commun. Eng. Mag.*, 2003, **1**, (5), pp. 14–17
7 Sibille, A., Bories, S.: 'Spatial diversity for UWB communications'. Fifth European Personal Mobile Communications Conf. (EPMCC), 2003, pp. 367–370
8 Ramirez-Mireles, F.: 'On the performance of ultra-wide-band signals in Gaussian noise and dense multipath', *IEEE Trans. Veh. Technol.*, 2001, **50**, (1), pp. 244–249
9 Farserotu, I., Hutter, A., Platbrood, F., Gerrits, I., Pollini, A.: 'UWB transmission and MIMO antenna systems for nomadic user and mobile PAN', *Wirel. Pers. Commun.*, 2002, **2**, (22), pp. 297–317
10 DErrico, R., Sibille, A., Giorgetti, A., Chiani, M.: 'Antenna diversity in UWB indoor channels'. IEEE Int. Conf. Ultrawideband (ICUWB 2008), Hanover, Germany, 10–12 September 2008, pp. 13–16
11 Molisch, A.F.: 'MIMO-UWB propagation channels'. 2010 Proceedings of the Fourth European Conf. on Antennas and Propagation (EuCAP), 12–16 April 2010, pp. 1–6
12 Li-Chun, W., Wei-Cheng, L., Kuan-Jiin, S.: 'On the performance of using multiple transmit and receive antennas in pulse-based ultrawideband systems', *IEEE Trans. Wirel. Commun.*, 2005, **4**, (6), pp. 2738–2750
13 Bengtsson, M.: 'From single link MIMO to multi-user MIMO'. IEEE Int. Conf. on Acoustics, Speech and Signal Procrocessing, 2004, vol. 4, pp. iv-697–iv-700
14 Al-Qaraawy, S.M., Ali, N.A.: 'Adaptation of BPSK/TH/UWB parameters using RAKE receiver with IPI in WPAN indoor multipath fading channels', *Eng. Technol.*, 2008, **26**, (11), pp. 1316–1325
15 Dong, S., *et al*: 'On the empirical evaluation of spatial and temporal characteristics of ultra-wideband channel'. IEEE 69th Vehicular Technology Conf., 2009, Barcelona, 26–29 April 2009, pp. 1–5
16 Sommerkorn, G., Richter, A., Thoma, R.S., Wirnitzer, W.: 'Antenna multiplexing & time alignment for MIMO channel sounding'. Twenty-seventh URSI General Assembly, Maastricht, NL, August 2002, pp. 28–29
17 Salous, S., Razavi-Ghods, N.: 'Semi-sequential MIMO channel measurements in indoor environments'. TD(04) 079, COST273 Meeting, Gothenburg, Sweden, June 2004, pp. 1327–1331
18 Bonek, E., Hofstetter, H., Mecklenbrauker, C.F., Steinbauer, M.: 'Double directional super-resolution radio channel measurements'. Thirty-ninth Annual Allerton Conf. Communication, Control and Computing, Illinois, USA, 2001, pp. 17–31
19 Thoma, R.S., Hampicke, D., Landmann, M., Sommerkorn, G., Richter, A.: 'MIMO measurement for double-directional channel modeling'. IEE Seminar on Communications Systems from Concept to Implementations, (Ref. No. 2001/175), 12 December 2001, pp. 1/1–1/7
20 Catherwood, P.A., Scanlon, W.G.: 'Measurement errors introduced by the use of co-axial cabling in the assessment of wearable antenna performance in off-body channels'. European Conf. on Antennas and Propagation 2011 (EuCAP), Rome, 11–15 April 2011, pp. 3787–3791
21 Dietrich, C.B., Dietze, K., Nealy, J.R., Stutzman, W.L.: 'Spatial, polarization and pattern diversity for wireless handheld terminals', *IEEE Trans. Antennas Propag.*, 2001, **49**, pp. 1271–1281
22 Clarke, R.H.: 'Statistical theory of mobile-radio reception', *Bell Syst. Tech. J.*, 1968, **47**, pp. 957–1000
23 Jakes, W.C., (Ed:), 'Microwave mobile communications' (IEEE Press, New York, 1974)
24 Saunders, S.R., Aragón-Zavala, A.: 'Antennas and propagation for wireless communication system' (John Wiley & Sons, UK, 2007)
25 Su-Nam, K., Chul-Yong, U., Dong-Wook, K., Ki-Doo, K.: 'A study on the wireless MIMO-UWB transceiving techniques for WPAN'. 2005 Digest of Technical Papers Int. Conf. on Consumer Electronics, 8–12 January 2005, pp. 91–92
26 Kafle, P.L., Intarapanich, A., Sesay, A.B., McRory, J., Davies, R.J.: 'Spatial correlation and capacity measurements for wideband MIMO channels in indoor office environment', *IEEE Trans. Wirel. Commun.*, 2008, **7**, (5), pp. 1560–1571
27 Cotton, S.L., Scanlon, W.G.: 'Measurements, modeling and simulation of the off-body radio channel for the implementation of body worn antenna diversity at 868 MHz', *IEEE Trans. Antennas Propag.*, 2009, **57**, (12), pp. 3951–3961
28 Al-Tamimi, H., Al-Qaraawy, S.M.: 'UWB propagation indoor statistical channel modeling'. ISECS Int. Colloquium on Computing, Communication, Control and Management (CCCM 2009), 8–9 August 2009, vol. 1, pp. 379–383
29 Ziri-Castro, K.I., Scanlon, W.G., Evans, N.E.: 'Prediction of variation in MIMO channel capacity for the populated indoor environment using a Radar cross-section-based pedestrian model', *IEEE Trans. Wirel. Commun.*, 2005, **4**, pp. 1186–1194
30 Fort, A., Ryckoert, J., Desset, C., *et al*: 'Ultra-wideband channel model for communication around the human body', *IEEE J. Sel. Areas Commun.*, 2006, **24**, (4), pp. 927–933
31 Molisch, A.F., Steinbauer, M.: 'Condensed parameters for characterizing wideband mobile radio channels', *Int. J. Wirel. Inf. Netw.*, 1999, **6**, (3), pp. 133–154
32 Kaiser, T., Feng, Z., Dimitrov, E.: 'An overview of ultra-wide-band systems with MIMO', *Proc. IEEE*, 2009, **97**, (2), pp. 285–312
33 Wong, S.S.M., Lau, F.C.M., Tse, C.K.: 'Propagation characteristics of UWB radio in a high-rise apartment'. The Eighth Int. Conf. on Advanced Communication Technology, 2006 (ICACT 2006), 20–22 February 2006, vol. 2, pp. 5–918
34 Chong, C., Youngeil, K., Seong-Soo, L.: 'A statistical based UWB multipath channel model for the indoor environments'. IEEE Intelligent Vehicles Symp. WPAN Applications, 6–8 June 2005, pp. 525–530
35 Jakes Jr. W.C.: 'A comparison of specific space diversity techniques for reduction of fast fading in UHF mobile radio systems', *IEEE Trans. VT-20*, 1971, **4**, pp. 81–92
36 Khaleghi, A.: 'Diversity techniques with parallel dipole antennas: radiation pattern analysis', *Prog. Electromagn. Res., PIER 64*, 2006, **1**, pp. 23–42
37 Vaughan, R.: 'Spaced directive antennas for mobile communications by the Fourier transform method', *IEEE Trans. Antennas Propag.*, 2000, **48**, (7), pp. 1025–1032
38 Bonek, E., Herdin, M., Weichselberger, W., Ozcelik, H.: 'MIMO – study propagation first!'. Proc. Third IEEE Int. Symp. on Signal Processing and Information Technology, 14–17 December 2003, pp. 150–153
39 Abbasi, Q.H., Alomainy, A., Hao, Y.: 'Antenna diversity technique for enhanced ultra wideband radio performance in body-centric wireless networks'. 2010 European Wireless Technology Conf. (EuWIT), 27–28 September 2010, pp. 197–200
40 Qiu, R.C., Chenming, Z., Zhang, J.Q., Nan, G.: 'Channel reciprocity and time-reversed propagation for ultra-wideband communications'. IEEE Antennas and Propagation Society Int. Symp., 9–15 June 2007
41 Gesbert, D., Akhtar, J.: 'Transmitting over ill-conditioned MIMO channels: from spatial to constellation multiplexing', in Kaiser, T., Bordoux, A., Boche, H. *et al.* (Eds). Smart Antennas: State of the Art, Hindawi Publishing Corporation, 2005, pp. 443–461
42 Mitic, A.M., Stefanonic, M.C.: 'Second order statistics of the signal in Rician-lognormal fading channel with selection combining'. Facta Universitatis Series: Electronics and Energetics (08/2007), August 2007
43 Molisch, A.F.: 'Wireless communications' (John Wiley & Sons, UK, 2011, 2nd edn.)
44 Malik, W.Q., Edwards, D.J.: 'Measured MIMO capacity and diversity gain with spatial and polar arrays in ultrawideband channels', *IEEE Trans. Commun.*, 2007, **55**, (12), pp. 2361–2370
45 Raímundo, X., Salous, S., Nasr, K.: 'UWB MIMO measurements in reverberation chamber and indoor environment', 2012 International Symposium on Signals, Systems and Electronics (ISSSE), 3–5 Oct. 2012, pp. 1–5

doi: 10.1049/iet-map.2011.0565